A model of phase transitions in the system of electro-optical dipolar chromophores subject to an electric field

Yuriy V. Pereverzev, Oleg V. Prezhdo,[a] and Larry R. Dalton
Department of Chemistry, University of Washington, Seattle, Washington 98195-1700

(Received 14 January 2002; accepted 21 May 2002)

An analytical model for the nonlinear behavior of the electro-optic (EO) coefficient in chromophore–polymeric materials is developed. The sharp decline of the EO coefficient above a threshold chromophore concentration is attributed to a second order phase transition transforming the chromophore dipolar system into an antiferroelectric state. The rise of antiferroelectric correlations between chromophore dipoles deteriorates the efficiency of the poling process aimed at achieving a noncentrosymmetric chromophore ordering by application of an electric field. The location of the phase transition and the magnitude of the EO coefficient are investigated as functions of molecular and thermodynamic parameters. Particularly remarkable observations are made regarding the dependence of the EO coefficient on the macroscopic shape of samples used for poling. Slab shaped samples that are common in practice are least efficient for the poling process. Any degree of sample elongation in the direction of the poling field shifts the antiferroelectric phase transition towards higher chromophore concentrations and radically increases the maximum value of the EO coefficient. The theory is applied to two chromophore systems that are typical of materials used in EO devices. Fine agreement with the experimental data is achieved with little adjustment. © *2002 American Institute of Physics.* [DOI: 10.1063/1.1493182]

INTRODUCTION

Organic materials with highly nonlinear optical (NLO) properties are finding numerous applications in photonic and electro-optic (EO) devices involving electrical-to-optical signal transduction, fiber-optic transmission lines, lasers, storage devices, flat panel displays, and biomedical voltage sensors.[1–10] NLO chromophores with electron donor and acceptor substituents possess large molecular dipole moments and hyperpolarizabilities, forming the basis for EO modulators that encode an electrical driving signal onto an optical transmission beam.[6–10] Higher speeds, wider bandwidths and lower drive-voltages in the chromophore based EO modulators are achieved through a systematic chemical design of chromophores. A typical chromophore is an asymmetric quasilinear conjugated molecule that carries a large dipole moment due to the presence of electron donor and acceptor groups at the ends and possesses a highly non-linear molecular polarizability. Combined with the acentric order of chromophores achieved in polymer matrices by application of an external electric poling field, the non-linear molecular polarizability results in a macroscopic EO response.

The required high macroscopic EO activity can be achieved in the chromophore-polymer materials by optimization of several types of properties. Further improvement of the NLO response of the chromophore–polymer systems and design of new materials proceed in two major directions. First, NLO parameters of individual chromophore molecules are investigated and optimized. Second, the acentric order of chromophores in polymer matrices is studied to enhance the macroscopic NLO response.

In simple terms, the optical nonlinearities appear as a result of the anharmonicity of the chromophore potential that drives the donor electron. For instance, the cubic anharmonicity of the chromophore potential with respect to the electron displacement is responsible for the doubling of the optical frequency and results in the Pockels effect that is linear in the electric field. The variation and optimization of the electronic anharmonicity are achieved with chromophores of different types and shapes using a diversity of electron donor and acceptor substituents.

The asymmetry of the chromophore electronic potential is a required but not a sufficient condition for an NLO device. A macroscopic asymmetry in the arrangement of the chromophores in the polymer matrix is also needed. The directions of the quasilinear chromophores have to be ordered in an appropriate manner. The forces that determine the chromophore ordering are due to the interactions both between the chromophores as well as with the electric field. These forces are capable of suppressing the disordering effect of the heat bath.

The chromophores are characterized by significant values of dipole moments. A typical value of the chromophore dipole is about 10 Debye. Since chromophores are quasilinear molecules, it may be assumed that the dipole moments point along the longest molecular axis. Electric polarization of the chromophore system produces the macroscopic asymmetry required for the NLO response. The electric polarization is achieved by application a poling field. The chromophore-poling field and chromophore-chromophore interactions are the key forces that determine the macroscopic

[a]Author to whom correspondence should be addressed. Electronic mail: prezhdo@u.washington.edu

asymmetry. Other types of molecular forces, such as the excluded volume or Gay–Berne interactions, have a secondary effect on the asymmetry. Forces of this type can determine the spatial or orientation order of the chromophore molecular axes. In the presence of only the excluded volume or Gay–Berne forces, the molecular arrangement remains centrosymmetric. The addition of the chromophore-poling field and chromophore–chromophore electrostatic interactions creates a macroscopic asymmetry.

The polarization of the chromophore–polymer system and, therefore, the macroscopic asymmetry and NLO response differ depending on the thermodynamic state of the chromophore dipoles. The thermodynamic parameters, such as chromophore concentration x and strength of the poling field E, can be manipulated in order to change the thermodynamic state and maximize the polarization. If the dipole–dipole interaction had only the ferroelectric component, an arbitrary polarization could have been created by increases in x and E. This does not happen, however. As shown experimentally in Refs. 6–9 for several fixed values of E, the EO coefficient that is closely related to the macroscopic polarization attains a maximum value as a function of x and rapidly decays with a further concentration increase. The eventual decay of the macroscopic polarization with increasing chromophore concentration appears due to the antiferroelectric component of the dipole–dipole interaction.[6–10]

Our earlier theoretical investigations[11–14] of the thermodynamic states of the systems of chromophore dipoles have been carried out under the assumption that the dipole–dipole interaction can be satisfactory described by an Ising model. The assumption has been made based on the fact that in the experimentally relevant concentration range the system of the quasilinear chromophores can be expected to order by the Gay–Berne forces into a nematic or a smectic state. In either state the chromophore axes are orientation ordered. In the presence of the orientation order the dipole–dipole interaction is naturally transformed into the Ising form. The concentration maximum of the EO coefficient has been described in the model[11–14] by the antiferroelectric phase transition in the dipolar system. Above the critical concentration the antiferroelectric state becomes more thermodynamically stable than the paraelectric state, and further concentration increases diminish the macroscopic asymmetry. For the chromophore dipole moment of about 10 Debye and the polymer dielectric constant on the order of one, the antiferroelectric component of the Ising model appears too strong. Due to the overestimation of the antiferroelectric interaction, the concentration maximum of the EO coefficient predicted by the Ising model is shifted towards lower chromophore concentrations compared to the experimental data.[11] The antiferroelectric component of the dipole–dipole interaction is suppressed by increase of the polymer dielectric constant ϵ, as shown in Ref. 11, or by displacement of the location of the chromophore dipole from the molecular center of mass and deviation of the dipole direction away from the chromophore longest molecular axis, as in Ref. 12.

In present, we explore another alternative that allows us to bring the antiferroelectric phase transition point predicted by the Ising model towards higher values of chromophore concentration and in agreement with the experiment. The number of states available for each chromophore dipole will be increased. The Ising model allows for only two states: up and down. The number of the available states can be increased assuming that the anisotropic Gay–Berne (or excluded volume) component of the chromophore-chromophore interaction has little effect on the dipolar ordering in the relevant concentration regime. In such case, the molecular axes of the quasilinear chromophores are not orientation ordered, and chromophore dipoles can point in any direction. An isotropic model of this kind is investigated in Ref. 10 by a Monte Carlo simulation and shows good agreement with experiment. An increasing number of possible states of chromophore dipoles shift the antiferroelectric transition towards higher chromophore concentrations. As shown below for the current model, the structure of the antiferroelectric state subject to the poling field is qualitatively different from that of the Ising model. The antiferroelectric state in the Ising model has a collinear structure with the dipolar sublattices pointing along the electric field. The chromophore dipoles of the antiferroelectric state of the isotropic model are positioned at an angle to the poling field.

The current study, similar to the Ising model studies[11,12] and particularly,[13] investigates the effect of the macroscopic sample shape on the thermodynamic states of the dipolar system. The effect emerges through the depolarization fields that are closely linked to the sample shape and appear in dipolar systems with the long-range interactions in the presence of macroscopic polarization. Due to the shape dependence of the macroscopic polarization and the antiferroelectric order parameter, the shape of a sample is capable of significantly shifting the value of the chromophore concentration at the phase transition. The concentration maximum of the EO coefficient coincides with the location of the phase transition and, as a result, the sample shape becomes an additional variable that can be tuned in order to optimize the NLO response. It should be noted that the shape of the sample is important only for chromophore ordering by poling. After chromophore order is locked by polymer cooling, the material can be processed into any shape with no change to its NLO response.

THEORETICAL MODEL

Unless chromophore molecules order into a liquid crystal phase within the relevant concentration range, the electric properties of the chromophore system that appear due to the dipole–dipole interaction cannot be described by an Ising model as in Refs. 11–13, and the full dipole–dipole Hamiltonian should be used instead,

$$H=\frac{\mu^2}{2\epsilon}\sum_{l\neq m}\frac{r_{lm}^2(\vec{\sigma}_l\cdot\vec{\sigma}_m)-3(\vec{r}_{lm}\cdot\vec{\sigma}_l)(\vec{r}_{lm}\cdot\vec{\sigma}_m)}{r_{lm}^5}-\frac{\mu E}{\epsilon}\sum_l \sigma_l^z. \quad (1)$$

Here, $\vec{\sigma}_l,\vec{\sigma}_m$ are the unit vectors that determine the directions of dipoles l,m of magnitude μ. For simplicity, the dipoles are assumed located on a simple cubic lattice. $\vec{r}_{lm}$ is the

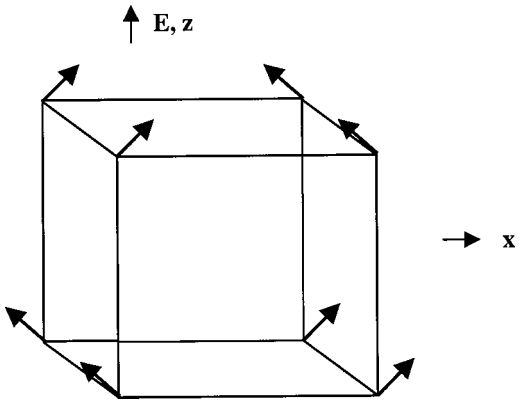

FIG. 1. Antiferroelectric structure on a simple cubic lattice.

radius vector between chromophores l and m. The axes of the coordinate system point along the cubic lattice axes. The external electric field E acts in the z direction.

The thermodynamic states of the chromophore system will be investigated in the presence of the dipole–dipole interaction described by Hamiltonian (1), assuming that the higher order interactions, such as the dipole-induced dipole and dispersive interactions, are less important for the electrostatic order. The experimental studies[6–9] of the EO coefficient as a function of the chromophore concentration indicate that the antiferroelectric dipole–dipole correlations substantially increase with increasing concentration. Based on this observation it is assumed that at some value of the chromophore concentration an antiferroelectric state is formed by a thermodynamic phase transition. The antiferroelectric state of a system of dipoles on a cubic lattice has a chain structure as was first established in Ref. 15. This reference also shows that in needle-shaped samples the ground state of systems of dipoles on body-centric and face-centric lattices is ferroelectric. As shown by Kittel[16] for sample shapes different from a needle, the ground state is inhomogeneous with many domains. A more detailed discussion of ferroelectric states in dipolar systems can be found in Refs. 17–19.

The antiferroelectric state of the current model is described by two ferroelectric chains belonging to different sublattices as have been done in Refs. 11 and 12. In contrast to the Ising model developed in these references, where the electric moments of the sublattices can point only along the electric field E, the electric moments of the sublattices in the present isotropic model are oriented at an angle to the field. A nonzero angle between the electric moments and the field lowers the thermodynamic potential corresponding to Hamiltonian (1). The antiferroelectric sublattices are localized in the (z,x) plane and are symmetric with respect to the z axis. The angle between the first sublattice and the z axis is denoted by $\theta_1=\theta$. The angle between the second sublattice and the z axis is $\theta_2=-\theta$. The antiferroelectric state with the ferroelectric chains pointing along the y axis is depicted in Fig. 1. Modifications to the antiferroelectric structure of Fig. 1 are not expected to change qualitatively the results obtained below. This conclusion follows from the phenomenological description of the antiferroelectric state, where its microscopic structure is averaged out.[20]

The electrostatic order in the above model is investigated in the self-consistent-field approximation that reduces the many-body problem to a one-particle description. In this approximation the dipole moment of a chromophore interacts both with the external field and with an effective field consisting of three contributions. These are the local field $\vec{E}_l$, the Lorentz field $\vec{E}_L$ and the depolarization field $\vec{E}_d$. The separation of the effective field acting on the selected dipole into the local, Lorentz and depolarization contributions is general for models that characterize dipolar systems in terms of average quantities,[21] including the current self-consistent mean-field model. Summation over the dipole–dipole interaction on a lattice is replaced in such models by integration over the volume of the sample. A formal replacement of summation to integration, however, leads to a divergence at zero of the radial coordinate. In order to avoid the divergence the summation is carried out explicitly over a small volume of the sample around the selected dipole. The explicit summation over the small volume gives the local field $\vec{E}_l$. The shape of the small volume is arbitrary, but is most conveniently chosen spherical, producing the so-called Lorentz sphere. The external field polarizes the bulk material generating surface charges both at the outside boundary of the sample and on the Lorentz sphere. The field produced by the surface charges at the boundary between the bulk and the Lorentz sphere is the Lorentz field $\vec{E}_L$. Changing the shape of the small volume changes the local and Lorentz fields in a consistent manner such that the resulting effective field remains the same. Ellipsoidal shapes are also typical and can be used depending on the dipole lattice. In general, selection of an appropriate shape for the small volume can improve convergence of the lattice sum of the local field, but can also lead to an anisotropic Lorentz field. Spherical shape is optimal for the cubic lattice, leading to a rapid convergence of the lattice sum that is accurately approximated by the interaction of the selected dipole with its nearest neighbors. The depolarization field $\vec{E}_d$ is produced by the surface charges at the outside boundary of the sample. The depolarization field depends on the macroscopic shape of the sample. In present, the macroscopic shape of the sample is described by a rotation ellipsoid with the rotation axis directed along the external field. The ellipsoid can be prolate or oblate producing different depolarization factors n within the range from zero for needle to one for slab.

Let σ_1, σ_2 denote the average values $\langle\sigma_{z1}\rangle$, $\langle\sigma_{z2}\rangle$ of the projections of the dipole moments selected from the first and second sublattices, correspondingly. The projections are taken in the coordinate systems associated with the sublattices, i.e., where the z_1 and z_2 axes point along the directions of the average dipole moments in each sublattice. Due to symmetry, $\sigma_1=\sigma_2=\sigma$. Consider the components of the effective field, first given in the coordinate system associated with the external field. The Lorentz $\vec{E}_L$ and depolarization $\vec{E}_d$ fields are determined by the average value of polarization in the dipole system. The system is polarized along the field and only the z components of the Lorentz and depolarization fields are present. Omitting for simplicity the z index, the sum of the two fields can be expressed as

$$E_L + E_d = -4\pi(n-1/3)\mu\sigma N\cos\theta. \tag{2}$$

Here, N is the number of chromophore molecules in a unit volume and n is the depolarization factor. The local fields acting on the dipoles in the first and second sublattices are calculated in the nearest-neighbor approximation. Only the x component of the local fields survives. The local field acting on the selected dipole of the first sublattice is

$$E_l = 8\mu\sigma N\sin\theta. \tag{3}$$

The full Hamiltonian acting on the selected dipole of the first sublattice in the self-consistent-field approximation is

$$H = -\frac{\mu E^*}{\epsilon}\sigma_z - \frac{\mu E_l}{\epsilon}\sigma_x, \tag{4}$$

where $E^* = E - 4\pi(n-1/3)\mu\sigma N\cos\theta$. It is convenient to rewrite Hamiltonian (4) in the coordinate system associated with the direction of polarization of the sublattice. The following coordinate transformation is used for this purpose:

$$\begin{aligned}\sigma_z &= \sigma_{z1}\cos\theta - \sigma_{x1}\sin\theta,\\ \sigma_x &= \sigma_{z1}\sin\theta + \sigma_{x1}\cos\theta.\end{aligned} \tag{5}$$

The transverse component of the effective field in Hamiltonian (4) is eliminated in the sublattice coordinate system. Based on this condition, the first of the two equations for the parameters σ and θ is obtained,

$$\sin\theta(8\mu\sigma N\cos\theta - E^*) = 0. \tag{6}$$

With (6) taken into account, Hamiltonian (4) acquires the following form in the sublattice coordinate system:

$$H = -\frac{\mu\tilde{E}}{\epsilon}\sigma_{z1}, \tag{7}$$

where $\tilde{E} = E^*\cos\theta + E_l\sin\theta$. It is straightforward to carry out the thermodynamic averaging of the operator σ_{z1} using the transformed self-consistent Hamiltonian (7). The averaging gives the second equation for the parameters σ and θ,

$$\sigma = \frac{\gamma\cosh\gamma - \sinh\gamma}{\gamma\sinh\gamma}, \quad \gamma = \frac{\mu\tilde{E}}{\epsilon T}. \tag{8}$$

It follows from Eq. (6) that the system of dipoles can exist in two thermodynamic states. In the first state $\theta = 0$, i.e., the sublattices are polarized along the external field. This state will be referred to as the paraelectric state. The average z projection of the chromophore dipole moment in the paraelectric state is given by

$$\sigma = \frac{\gamma - \tanh\gamma}{\gamma\tanh\gamma}, \quad \gamma = [e - \pi(n-1/3)x\sigma\eta]/\epsilon, \tag{9}$$

where $e = \mu E/T$ and $x = N/10^{20}$ are the reduced electric field and chromophore concentration, respectively. N is the chromophore number density, and $\eta = 4\mu^2 10^{20}/T$. In the second state, the direction of the sublattice polarization deviates from the direction of the external field. The angle between the polarization and the field equals

$$\cos\theta = \frac{e}{2\sigma\eta x[1 + (n-1/3)\pi/2]}. \tag{10}$$

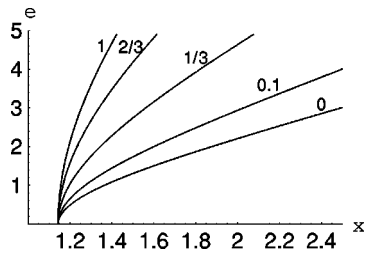

FIG. 2. Phase transition lines in the chromophore concentration x and electric field e coordinates obtained for different values of the depolarization factor n, ranging from 0 for needle to 1/3 for sphere and 1 for slab. The disordered paraelectric state region is located to the left of the line, while the ordered antiferroelectric state is to the right of the line. The antiferroelectric state region is decreased for prolate samples.

This is the antiferroelectric state. In the antiferroelectric state the average projection of the chromophore dipole on the direction of the sublattice polarization is given by

$$\sigma = \frac{\gamma - \tanh\gamma}{\gamma\tanh\gamma}, \quad \gamma = 2\eta\sigma x/\epsilon. \tag{11}$$

It follows from Eq. (11) that σ in the antiferroelectric state is independent of both the external field and the macroscopic shape of the sample.

Within the space of the external parameters, including chromophore concentration, strength of the electric field, temperature, etc., the regions of para- and antiferroelectric states are separated by a second order phase transition surface. The equation for the phase transition surface can be easily found, if the phase transition is approached from the antiferroelectric side, and θ is set to 0:

$$\begin{aligned}x &= \frac{\epsilon\gamma^2\tanh\gamma}{2\eta(\gamma - \tanh\gamma)},\\ \gamma &= \frac{e}{\epsilon[1 + \pi(n-1/3)/2]}.\end{aligned} \tag{12}$$

The theory developed here is applied below in order to investigate polarization of the chromophore system and the macroscopic NLO coefficient as functions of the molecular and thermodynamic parameters. The theoretical results are compared with the experimental data for two typical chromophore–polymer systems.

RESULTS AND DISCUSSION

The results of the current study indicate that the EO coefficient reaches maximum at the antiferroelectric phase transition. Therefore, it is necessary to predict the location of the phase transition as a function of the external parameters. Figure 2 depicts phase transition lines calculated in the concentration-poling field (x,e) coordinate system according to Eq. (12) for $T = 373$ K, $\mu = 13$ D, $\epsilon = 1$ and several values of the depolarization parameter n characterizing the shape of the poled sample. The system exists in the paraelectric state to the left of the phase transition curve. The ordered antiferroelectric state is thermodynamically stable to the right of the curve. All curves start at $e = 0$ and $x_0 = 1.5\epsilon/\eta$. Increases of temperature and polymer dielectric constant shift the starting

point to the right. Larger chromophore dipoles decrease x_0. In the case considered in Fig. 2 the value of x_0 is 3 times larger than the corresponding value in the Ising model,[11] i.e., the antiferroelectric phase transition is observed at higher chromophore concentrations. Figure 2 demonstrates a strong dependence of the location of the phase transition on the macroscopic sample shape. The ordered state region is significantly reduced for needle ($n=0$) compared to slab ($n=1$). Correspondingly, the favorable paraelectric region is enlarged.

As a result of the phase transition, the thermodynamic characteristics of the chromophore system change their dependence on the external parameters. In particular, consider the total polarization combined over the two sublattices with the only nonvanishing z-component p_z and the EO coefficient r. The latter has been measured for several types of chromophore systems and reported in Refs. 6–10. Polarization p_z is defined for a single chromophore relative to the absolute magnitude of the chromophore dipole. Polarization in the paraelectric state is given by

$$p_z=\sigma, \tag{13}$$

i.e., p_z is fully determined by Eq. (9). In particular, it follows that p_z of spherical samples is independent of concentration x. Polarization in the antiferroelectric state is determined by Eqs. (10) and (11) and equals

$$p_z=\sigma\cos\theta=\frac{e}{2\eta x[1+\pi(n-1/3)/2]}. \tag{14}$$

In the antiferroelectric state, p_z decreases with concentration by the inverse x^{-1} law. The concentration dependence of paraelectric (13) and antiferroelectric (14) polarizations is illustrated in Fig. 3 for different values of E and n. The largest polarization is achieved in needle-shaped samples. Slabs show the smallest polarization. In the paraelectric state, p_z grows as a function of concentration for prolate samples with $0\leqslant n<1/3$ and decreases for oblate samples with $1/3<n\leqslant 1$. In the antiferroelectric state, p_z decreases with concentration for all sample shapes. It should be emphasized that p_z is defined per dipole. The macroscopic polarization of the whole sample depends on concentration additionally through the growing number of dipoles.

The EO coefficient r is the central characteristic of the systems under study, since it determined the NLO response of chromophore–polymer materials in EO applications.[6–14] Of interest is the functional dependence of r on chromophore concentration, strength of the poling field and temperature. Taking into account the symmetry of the system, the normalized EO coefficient can be expressed in the self-consistent-field approximation by the parameters of either of the two sublattices

$$r=x\langle\sigma_z^3\rangle. \tag{15}$$

Expression (15) takes the following form in the transformed coordinate system, Eqs. (5):

$$r=x[\langle\sigma_{z1}^3\rangle\cos^2\theta+1.5(\langle\sigma_z\rangle-\langle\sigma_{z1}^3\rangle)\sin^2\theta]\cos\theta, \tag{16}$$

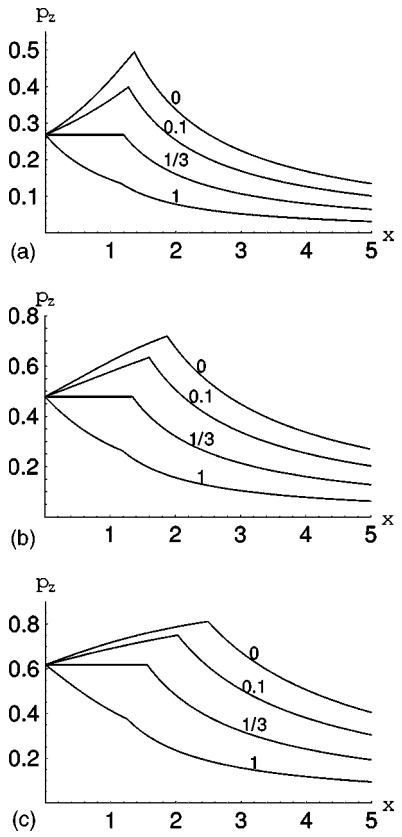

FIG. 3. Polarization per dipole p_z, Eqs. (13) and (14), as a function of dipole concentration x in samples of different shapes specified by the depolarization factor n. Three typical values of the external field are considered: (a) $e=1$, (b) $e=2$, (c) $e=3$ in reduced units, Eq. (9). The paraelectric state polarization increases with concentration for prolate samples ($n>1/3$), decreases for oblate samples ($n<1/3$), and is independent of concentration for sphere ($n=1/3$). In the antiferroelectric state the polarization always decreases with increasing concentration.

where the averaging is carried out with Hamiltonian (7).

The dependence of r on the external parameters is different for the para- and antiferroelectric states. In the paraelectric state with $\theta=0$ the averaging in (16) leads to the following expression:

$$r=x\frac{\sigma(\gamma^2+6)-2\gamma}{\gamma^2}, \tag{17}$$

where σ and γ are defined in Eq. (9). In the ordered state $\theta\neq 0$ and Eq. (16) takes the form

$$r=x\frac{\cos\theta}{\gamma^2}\{[\sigma(\gamma^2+6)-2\gamma]\cos^2\theta+3(\gamma-3\sigma)\sin^2\theta\}, \tag{18}$$

where θ, σ, and γ are defined in Eqs. (10) and (11).

Figure 4 illustrates the concentration dependence of the EO coefficient calculated by Eqs. (17) and (18) for various external fields and sample shapes. The data are calculated for chromophores with the dipole moment of $\mu=13$ D, for temperature $T=373$ K, and polymer dielectric constant $\epsilon=1$. Similar to polarization, the EO coefficients of prolate samples are greater than those of oblate samples. The maximum and minimum of r are attained in needle and slab,

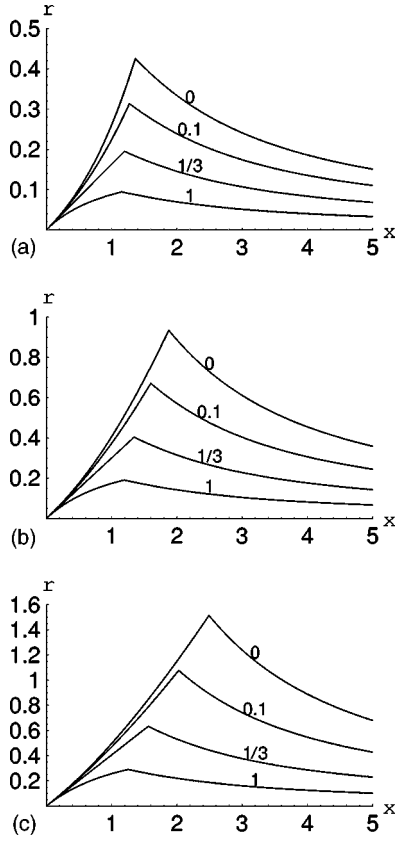

FIG. 4. EO coefficient r, Eqs. (17) and (18), as a function of chromophore concentration x in samples of different shapes subject to the poling field (a) $e=1$, (b) $e=2$, (c) $e=3$ in reduced units, Eq. (9). Both stronger fields and elongated samples increase the EO coefficient.

respectively. The data indicate that the EO coefficient can be maximized not only by increases in the external field, but also by elongation of the macroscopic sample.

The EO coefficient reaches its maximum value r_m at the phase transition point. The dependence of r_m on the external parameters can be obtained from Eq. (17), considering that at the phase boundary

$$\sigma=\frac{\epsilon}{2\eta x} \tag{19}$$

and that γ and x are related to e according to Eq. (12). It follows that

$$r_m=\frac{\epsilon}{2\eta\gamma}\left(\gamma^2+6-\frac{2\gamma^2\tanh\gamma}{\gamma-\tanh\gamma}\right). \tag{20}$$

The expressions for r_m in the weak and strong field limits are obtained from Eq. (20) by taking the $\gamma\ll 1$ and $\gamma\gg 1$ limits, respectively,

$$r_m(\gamma\ll 1)=\frac{3\epsilon\gamma}{10\eta}, \tag{21}$$

$$r_m(\gamma\gg 1)=\frac{\epsilon\gamma}{2\eta}. \tag{22}$$

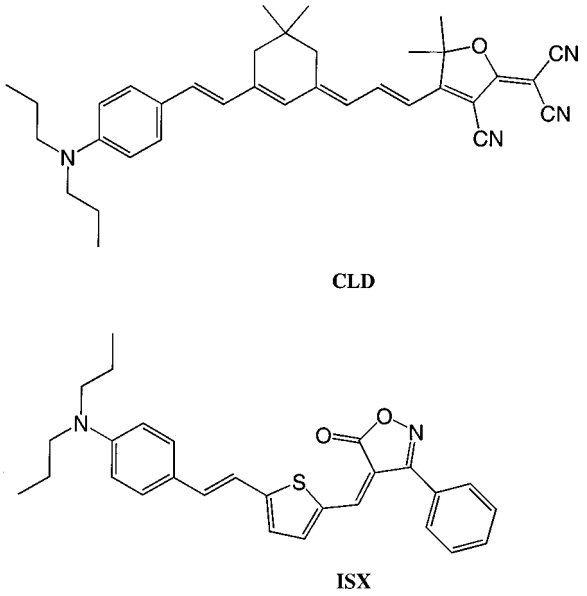

FIG. 5. Chemical structures of the CLD and ISX chromophores that are typical in NLO applications.

The EO coefficient r_m is linearly proportional to the field both in the weak and strong field limits. The proportionality coefficients are different, though. The EO coefficient grows faster in strong fields than in weak fields.

Finally, compare the theoretical dependence of the EO coefficient on chromophore concentration with the experimental data reported in Refs. 6–10. The comparison is made for the isoxazolone (ISX) and phenyltetraene-based (CLD) chromophores shown in Fig. 5. Since the experiments have been performed with slabs, the depolarization factor n used in Eqs. (17) and (18) is set to 1. A good agreement with the experimental data (circles) is achieved, Figs. 6(a) and 6(b). The theoretical line presented in Fig. 6(a) for the CLD system is obtained with the value of the chromophore dipole $\mu=13.47$ D reported in Refs. 6–10 and the polymer dielec-

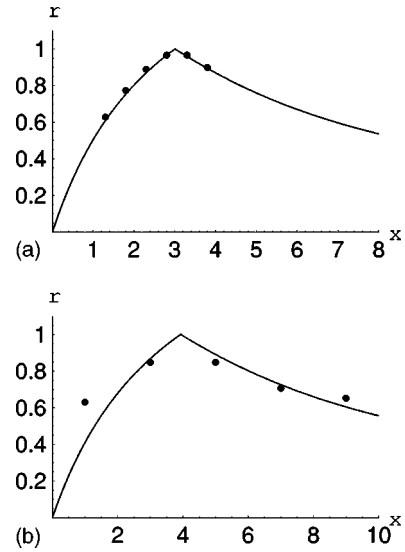

FIG. 6. Comparison between the experimental (circles) and theoretical (lines) data for (a) CLD and (b) ISX chromophore systems.

tric constant $\epsilon = 2.82$. It is interesting to note that the data are quite stable with respect to a variation in the chromophore and polymer properties. A theoretical curve visually identical to that of Fig. 6(a) is obtained for $\epsilon = 1$ and $\mu = 8$ D. Figure 6(b) presents the theoretical and experimental data for the ISX system. The theoretical data shown in Fig. 6(b) is calculated for $\epsilon = 1.3$ and $\mu = 8\ \mathrm{D}^{6-10}$ and is visually reproduced with $\epsilon = 1$ and $\mu = 7$ D.

CONCLUSIONS

In summary, the asymmetric order of dipolar chromophores in polymeric NLO materials has been investigated as a function of chromophore, polymer and external thermodynamic parameters. An analytical mean-field model has been developed to rationalize the nonlinear dependence of the dipole ordering and magnitude of the EO coefficient on chromophore concentration, strength of the external poling field, and, most strikingly, the geometric shape of the sample. It has been found that the experimentally observed leveling off and a subsequent sharp decrease of the EO coefficient with increasing chromophore concentration is attributed to antiferroelectric correlations between chromophore dipoles that neutralize the action of the poling field.

An antiferroelectric phase transition in the chromophore dipole system can occur without an external field. Increases of temperature and polymer dielectric constant shift the phase transition point to higher chromophore concentrations, while larger chromophore dipoles give the opposite effect. Compared to the Ising model,[11–13] the phase transition in the current isotropic model takes place at significantly higher concentrations. Application of the poling field delays the phase transition.

A strong dependence of the location of the phase transition on the macroscopic sample shape is observed. The antiferroelectric state region is significantly reduced for needle compared to slab. In addition, inside each of the para- and antiferroelectric state regions the largest polarization of the chromophore dipole is achieved in needle-shaped samples and the smallest one in slabs. In the paraelectric state, the chromophore polarization grows as a function of concentration for prolate samples and decreases for oblate samples. In the antiferroelectric state, the polarization decreases with concentration for all sample shapes.

Similar to polarization, the EO coefficients of prolate samples are greater than those of oblate samples. The largest and smallest coefficients are attained in needle and slab, respectively. The dependence of the EO coefficient on the external parameters is different for the para- and antiferroelectric states. The maximum of the EO coefficient is always observed at the phase transition point, and its value is linearly proportional to the strength of the poling field both in the weak and strong field limits. The proportionality coefficients are different in the two limits. The coefficient is larger for strong fields.

The developed model has been applied to the CLD and ISX chromophore systems that are typical of the chromophore–polymer EO materials. The theoretical results are stable to small variations in the chromophore and polymer properties and agree well with the experiment.

ACKNOWLEDGMENTS

O.V.P. is a Dreyfus New Faculty and Alfred P. Sloan Fellow. The work reported here has been supported by grants from National Science Foundation and Office of Naval Research.

[1] *Nonlinear Optical Properties of Organic and Polimeric Materials*, edited by D. J. Williams, ACS Symp. Ser. 233 (American Chemical Society, Washington, DC, 1983).
[2] S. R. Marder, L.-T. Cheng, B. G. Tiemann, A. C. Friedli, M. Blanchard-Desce, J. W. Perry, and J. Skindhoj, Science **263**, 511 (1994).
[3] F. Hide, B. J. Schwartz, M. A. Diaz-Garcia, and A. J. Heeger, Synth. Met. **91**, 35 (1997).
[4] I. G. Voigt-Martin, G. Li, U. Kolb, H. Kothe, A. V. Yakimanski, A. V. Tenkovtsev, and C. Gilmore, Phys. Rev. B **59**, 6722 (1999).
[5] J. Cornil, D. Beljonne, J. P. Calbert, and J. L. Bredas, Adv. Mater. **13**, 1053 (2001).
[6] A. W. Harper, S. Sun, L. R. Dalton, S. M. Garner, A. Chen, S. Kalluri, W. H. Steier, and B. H. Robinson, J. Opt. Soc. Am. B **15**, 329 (1998).
[7] B. H. Robinson, L. P. Dalton, A. W. Harper *et al.*, Chem. Phys. **245**, 35 (1999).
[8] A. K. Y. Jen, Y. Q. Liu, L. X. Zheng, S. Liu, K. Y. Drost, Y. Zhang, and L. R. Dalton, Adv. Mater. **11**, 452 (1999).
[9] Y. Shi, C. Zhang, H. Zhang, J. H. Bechtel, L. R. Dalton, B. H. Robinson, and W. H. Steier, Science **288**, 119 (2000).
[10] B. H. Robinson and L. R. Dalton, J. Phys. Chem. A **104**, 4785 (2000).
[11] Y. V. Pereverzev and O. V. Prezhdo, Phys. Rev. E **62**, 8324 (2000).
[12] Y. V. Pereverzev, O. V. Prezhdo, and L. R. Dalton, Chem. Phys. Lett. **340**, 328 (2001).
[13] Y. V. Pereverzev, O. V. Prezhdo, and L. R. Dalton, Phys. Rev. B **65**, 052104 (2002).
[14] O. V. Prezhdo, Adv. Mater. **14**, 597 (2002).
[15] J. M. Luttinger and L. Tisza, Phys. Rev. **70**, 954 (1946).
[16] C. Kittel, Phys. Rev. **82**, 965 (1951).
[17] S. H. L. Klapp and G. N. Patey, J. Chem. Phys. **115**, 4718 (2001).
[18] S. T. Lagerwall, J. Phys.: Condens. Matter **8**, 9143 (1996).
[19] P. I. C. Teixeira, J. M. Tavares, and M. M. Telo da Gama, J. Phys.: Condens. Matter **12**, R411 (2000).
[20] I. Musevic, R. Blinc, and B. Zeks, *The Physics of Ferroelectric and Antiferroelectric Liquid Crystals* (World Scientific, Singapore, London, 2000).
[21] C. Kittel, *Introduction to Solid State Physics* (Wiley, New York, 1996).